

Neuron Interference: Evidence-Based Batch Effect Removal

Matthew Amodio¹ Ruth Montgomery^{2*} Jenna Pappalardo^{2*} David Hafler^{2*} Smita Krishnaswamy^{2,1}

Abstract

New technologies such as single-cell RNA sequencing and mass cytometry are measuring cellular populations in high dimensions, offering unparalleled insights into cellular behavior and enabling new scientific discoveries. However, when these measurements are applied to multiple samples or experimental conditions, the resulting systematic variations, or *batch effects*, confound biological variation and create a vexing problem in comparing cellular populations. Moreover, these batch effects, which arise as a result of changed environmental condition, instrument variation, machine calibration, or human handling differences, can be complex and highly non-linear transformations. Despite their ubiquity, there are few computational tools designed to correct generally for such effects while maintaining biological differences. The ones that exist hold strong assumptions (such as linear shifts between batches).

Here, we propose an entirely novel approach to disentangling biological from batch variation where we take a specific subpopulation of cells as a control between the batches. This subpopulation can be an unchanged population (known via prior biology) or a repeatedly measured spike-in. We use an autoencoder to model the variation in the control, and then interfere with neuron activations on inference to correct for these differences on the entire sample. This technique, which we term *neuron interference*, is unique in its ability to generalize a batch effect learned on a subpopulation to the entire population.

1. Introduction

As biological researchers, our ability to make tremendous new discoveries is in large part facilitated by improvements in data acquisition with new instruments that can generate

more measurements per observation, more observations per subject, and more subjects per experiment than ever before. As promising as these technologies are, they come with a major limitation: *batch effects*. Batch effects are technical artifacts in the data that arise from our not being able to replicate experimental conditions exactly. The observed data can be affected by many factors such as the humidity in the laboratory, the calibration of the measuring instrument, the quality control on a purchased lot of reagent, and exactly how much reagent a technician pipetted into each well. Because our experiments cannot measure everything of interest in one run of the instrument, the datasets from each run must be combined and analyzed together despite the variability from these other sources.

Existing approaches to analyzing this combined data include removing observations determined to be unreliable or combining the results of separate analyses for each batch with meta-analysis [1, 2, 3]. Another approach is to use a statistical alignment model to remove differences between the samples. For example, one alignment model based on canonical correlation analysis maps both batches to a latent space, assuming a linear latent direction through the genes [4]. A mutual nearest neighbors alignment model imposes the very strong assumption that the shape of the data in each batch is the same and the batch effect shifts are orthogonal to the direction of the data [5]. An alignment model matching the mean and variance for each dimension of each batch imposes the assumption that all differences in the first two moments are batch effects and no differences in higher moments are batch effects [6]. Not only do these methods depend on strong assumptions in order to align the batches, but they then also attempt to remove all differences that fit their models of variation.

Instead of assuming that all variation that takes a specific form is a batch effect, and conversely that all batch effects take that form, we propose using an evidence-based method for learning a batch effect model from real data. To do this, we can use a *control*, or an invariant subpopulation that is measured in each *sample* of interest [7, 8, 9, 10, 11]. While the observed changes in the control offer the potential for differentiating between true and technical variation in the sample, it is a challenge to use this information to correct non-controls because batch effects can be highly non-linear, non-uniform in the space, and different in each sample [12].

*Equal contribution ¹Department of Computer Science, Yale University ²Department of Genetics, Yale University. Correspondence to: Matthew Amodio <matthew.amodio@yale.edu>.

The complexity of the task suggests that neural networks may be the right approach. However, there are fundamental difficulties in using neural networks for this task. A naive approach might be to train a network to map from one batch’s control to the other batch’s control and then apply it to the first batch’s sample. A neural network that is trained on only controls generally cannot map from the first batch sample to the second batch sample, i.e., there is an inherent out-of-sample extension issue. Neural networks will generally not automatically map to or from spaces in which they have not been trained on. Thus when a neural network is fed a data point from the non-control portion of the data it may map it to the nearest control point or to random noise.

Likewise, another naive approach might be to use regularizations to balance accurate reconstruction of the data and minimization of the variation between batches. This would not distinguish between batch variation and true biological variation, though, and remove the very signal we want to model as well as the technical noise. In addition to this problem, producing accurate reconstructions and producing data without its batch effects are opposite goals. The minimum of the sum of these two loss terms need not lead to the most desirable result: sacrifice reconstruction accuracy to completely remove batch effects, but otherwise maximize reconstruction accuracy. Instead, the minimization might be optimal with partially removed batch effects and partially preserved reconstruction.

To circumvent these issues of training, we propose modeling batch variation during *inference*. We simply train a standard autoencoder to map the entire dataset to itself and afterwards learn which neuron activations strongly encode for batch differences between controls. We take these neurons and realign their activations on inference without further training, using a process that we term *neuron interference* to match activations with each other. Thus we learn the networks internal model of batch effect from controls and use it to correct all datapoints.

Inference has been generally overlooked in the research community, with only rare discussions about computational efficiency or model interpretation [13]. To the best of our knowledge, there have been no attempts to use inference techniques to model the phenomenon of interest (in this case, batch effects).

We harness neuron interference for removing batch effect variation while preserving true biological variation because of several critical properties. With neuron interference, we can model highly complex variation. We can identify distinct sources of variation and selectively remove some but not others. We can learn an interference model on one population and meaningfully generalize it to a different population. These properties are essential and arise from using

a deep learning inference model.

The contributions of this work can be summarized as follows:

1. The introduction of the neuron interference inference algorithm for alignment
2. A framework for using neuron interference to correct batch effects in biological data
3. Extensive experimental validation on our real-world biological data

In the rest of this paper, we start by detailing the neuron interference algorithm. We then offer a brief validation of neuron interference on the classic MNIST dataset. Finally, we perform extensive demonstration of the effectiveness of neuron interference on our real mass cytometry and single-cell RNA sequencing data.

2. Model

2.1. Neuron interference

The neuron interference algorithm presented here operates during inference of an already trained autoencoder [14]. The process (summarized in Figure 1) extracts a hidden layer of the network, finds a neuron that has detected a feature associated with the difference between two batches, transforms that neuron’s activations for one batch to match that neuron’s activations for the other batch, and then feeds forward the new hidden layer with that neuron transformed (without further training).

Let $X \in \mathbb{R}^D$ be the data with $X_{ij}, i = 1 \dots N, j = 1 \dots D$ the value in the j^{th} dimension of the i^{th} observation. Let $l_i \in \{0, 1\}$ be the binary batch label of the i^{th} observation. Let h_{ij} be the activation of neuron j for observation i in the layer designated for neuron interference. Then we call the distribution of activations for each batch for a particular neuron the neuron distribution, i.e.:

$$ND_{jl} = \{h_{ij} : l_i = l\}$$

Neuron interference is a monotonic function that approximately aligns ND_{j0} and ND_{j1} by operating piecewise over the support, shifting points in the p^{th} percentile of ND_{j1} by $(\text{Percentile}_p(ND_{j0}) - \text{Percentile}_p(ND_{j1}))$. As a result, it takes as input ND_{j0} and ND_{j1} and returns a transformed ND'_{j1} such that the percentiles of ND'_{j1} and ND_{j0} are identical and the order of the points in ND_{j1} is preserved.

This nonparametric transformation ensures that the neuron distributions are approximately aligned without having to make any assumptions on their form.

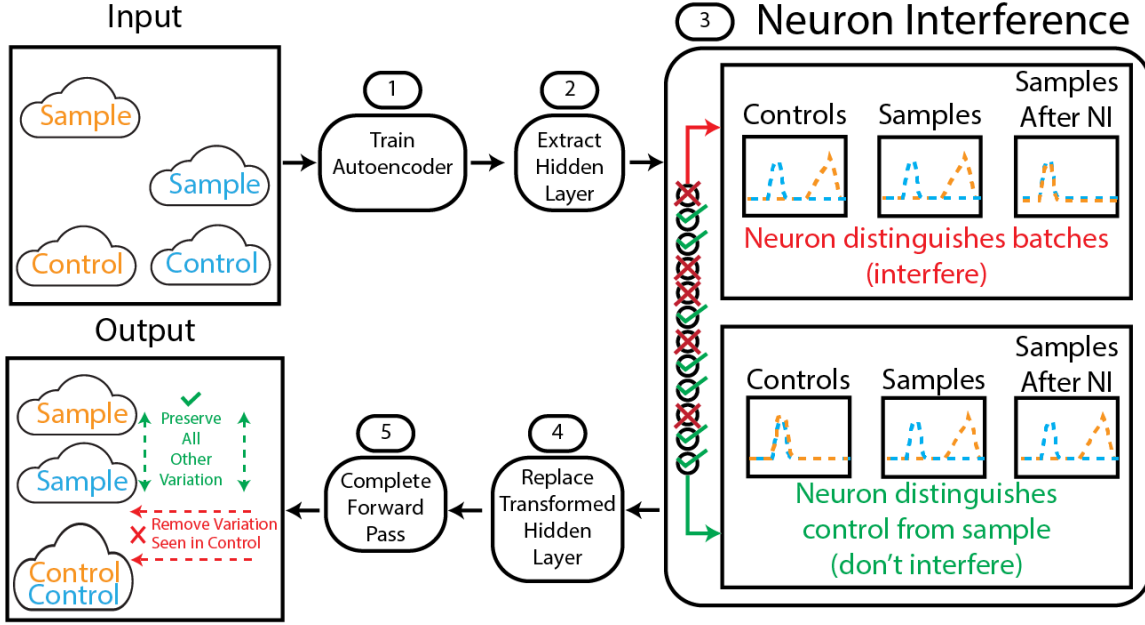


Figure 1. The samples have both technical (horizontal) and biological (vertical) variation. We use the control (which is repeatedly measured in each batch) to calibrate the samples for that batch. Neurons to interfere are identified by their differential activations in the *controls* across each batch. Differential firing in just the *sample* indicates true biological variation to be preserved. After neuron interference (NI), the samples have technical variation removed but biological variation preserved.

2.2. δ criterion for batch correction

The effectiveness of our method depends on an informed criterion for deciding whether the variation introduced by a given neuron is technical or truly biological. We look for neurons where the control and sample activate similarly to each other in both batches, but is different between batches. Such a feature is thus only separating batches rather than distinguishing amongst different points within a batch.

Let X^c and ND_{jl}^c denote the data and neuron distribution for neuron j and batch l for all observations in the control respectively, and X^s and ND_{jl}^s similarly for all observations in the sample. Our method for performing batch correction works by (a) identifying all neurons j whose ND_{j0}^c and ND_{j1}^c match a criterion for batch effects (b) performing neuron interference on ND_{j0}^s and ND_{j1}^s and (c) obtaining batch corrected data \tilde{X}_1^s by completing the networks forward pass on transformed neurons $ND_{j1}^{s'}$.

The criterion we choose to identify this, δ , uses the EMD (earth movers distance) [15] as a distance between two distributions:

$$\delta = (\delta_0 < 1) \wedge (\delta_1 < 1)$$

$$\delta_l = \frac{EMD(ND_l^s, ND_l^c)}{\min(EMD(ND_0^c, ND_1^c), EMD(ND_0^s, ND_1^s))}$$

This criterion identifies neurons as encoding batch effect if

each control/sample is closest to the control/sample from the same batch. By choosing to scale by the smaller of the distance between controls or the distance between the samples and using a threshold of 1, we avoid forcing the modeler to make the difficult decision of what a small EMD value is for the given dataset, or more likely, tune another hyperparameter. In the next section, we present our argument for using the δ criterion as a principled way of defining batch effects and examine distributions that are identified as batch effect and non-batch effect (Figure 4).

3. Experiments

3.1. MNIST

We first use the canonical MNIST dataset to demonstrate neuron interference's ability to align two data distributions by aligning internal neuron distributions. Initially, a three-layer convolutional autoencoder with stride 2, kernel size 4, leaky ReLU activation, and filter sizes 8–16–32–32–16–8 is trained on the entire dataset. After training, taking the first batch to be the class of 3's and the second batch to be the class of 8's, we rank the neurons in the last hidden layer in descending order of our criterion δ . Then, we perform neuron interference on an increasing number of neurons and complete the forward pass on the transformed neurons. We note performing neuron interference on the top $x\%$ of neurons by NI_x . Figure 2 shows an image of a 3

gradually becoming an image of an 8, with the top part of the image forming first faintly and then fully, followed by the bottom part in turn. Repeating this with different classes illustrates that the neuron interference inference method (a) successfully identifies the neurons responsible for creating the differences between any two classes (b) transforms the neurons in such a way that a forward pass on the altered neurons yields meaningful output (c) yields interpolated output that is partially between the two classes.

3.2. Mass cytometry

In the previous section, we demonstrated neuron interference gradually aligning output between two batches. In this section, we show how this can be used for removing batch effects in real biological experiments. To generate this data, we ran a mass cytometry experiment with cells from two different subjects. Mass cytometry measures the abundance of protein markers in individual cells by conjugating antibodies to known metals which can then be detected with mass spectrometry. Our two samples were run separately on different days, and the process involves calibrating the complex cytometry machine, carefully thawing and prepping the samples, and physically pipetting the amount of reagent that will measure each marker for the panel. Each of these steps affects the resulting measurements and even our best technicians are unable to precisely replicate the conditions over multiple runs.

With each sample, we measured an identical control, which we can now use to calibrate the differences in the two samples. Thus, we have a first sample, a second sample, the control measured with the first sample, and the control measured with the second sample. All four datasets are in \mathbb{R}^{35} , with the number of cells being 56000, 95000, 19000, and 23000, respectively. The data was preprocessed with a hyperbolic sine transformation.

For this experiment, the autoencoder had layers of size 3500–1750–100–1750–3500, was trained for 50 epochs on minibatches of size 100, and optimized with Adam using a learning rate of .001. We note that neuron interference operates exclusively on inference and is thus independent of these training choices. Here, our architecture differs from a vanilla autoencoder in one additional way that is customized to mass cytometry. The neuron interference layer, which directly precedes the output layer, is not fully connected to the output layer. Instead, we leverage the knowledge that batch effects act independently on the measurement of each marker by partitioning the final layer so that each neuron only contributes to the output of one dimension. That is, if the data exists in D dimensions and the network has n neurons connected to each output node, then dimension d_i is connected only to neurons $n_{\{j|j\in[i*n,(i+1)*n]\}}$. This ensures that if a neuron detects a batch effect in one dimen-

sion, interfering with that neuron only changes the data in that particular dimension. Crucially, though, the features the neurons learn to detect are dependent on the full representation of the data since all previous layers are fully connected. This is due to the fact that the previous layer is determined by looking at the full input space, and each neuron in the neuron interference layer must operate on this shared representation.

Neuron interference To evaluate neuron interference’s effect in detail, we visualize cells in the two-dimensional interferon gamma-chemokine receptor 6 (InfG-CCR6) space. Figure 3a shows the original raw data in this space, where the first batch differs from the second batch biologically in terms of CCR6, but artificially in terms of InfG. Thus we want to preserve the difference in CCR6 while eliminating the difference in InfG, which is technical artifact. We see that the δ criterion works here because the first batch’s controls differ from the second batch controls *only* in InfG. Neuron interference can leverage this information to correct the batch effect along the InfG axis while preserving the difference in the samples in CCR6. Methods that don’t use the information of the controls have no way of distinguishing between the two differences and have to either remove them both or preserve them both.

After neuron interference, InfG measurements for the first batch controls are shifted downward (Figure 3b) and the controls are thoroughly mixed, as should happen given they are identical physically. The first batch samples are also shifted downward along the InfG axis, but crucially, the signal that differentiates the two samples in CCR6 abundance is preserved.

We explore how uniformly applying the δ criterion selects only neurons to transform that correspond to batch effects by looking in detail at two neurons: one that outputs to InfG that is corrected and another that outputs to CCR6 that is preserved.

Corrected neuron Figure 4 shows the corrected neuron activating identically between the first batch samples and the first batch controls and likewise within the second batch. As such, both δ_0 and δ_1 are near zero, and this neuron is corrected. When viewed in the InfG-CCR6 space in Figure 4, we see that this neuron activates only in cells that are at the uppermost end of the InfG axis, and does so for both the samples and controls. Because these higher values of InfG are strongly associated with batch, the result of neuron interference for InfG is that the cells in the first batch are pulled towards those in the second batch (Figure 3). By automatically finding this neuron with our criterion and performing neuron interference, we were able to make a nonlinear transformation that was specific to one marker and operated piecewise on only part of the space.

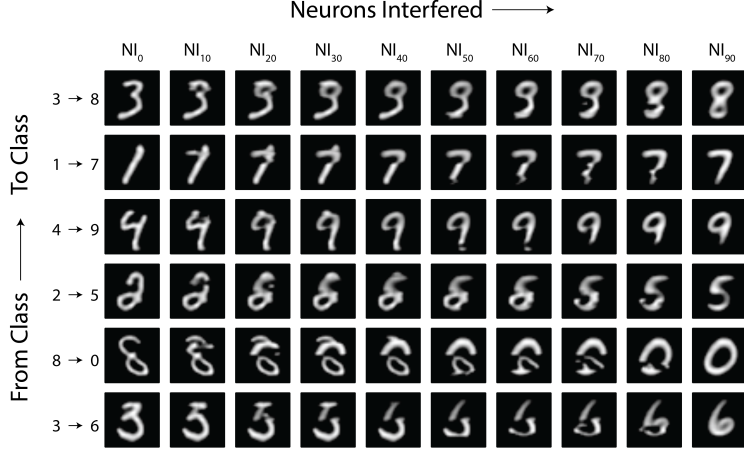


Figure 2. Neuron interference on MNIST. Performing neuron interference on an increasing number of neurons (ranked by their δ criterion) gradually transforms an image of any one class to an image of any other. Interference on 0% of the neurons leaves the point untouched, and interference on 100% of the neurons completely transforms it. Importantly, values in the middle are interpretable interpolations along the way.

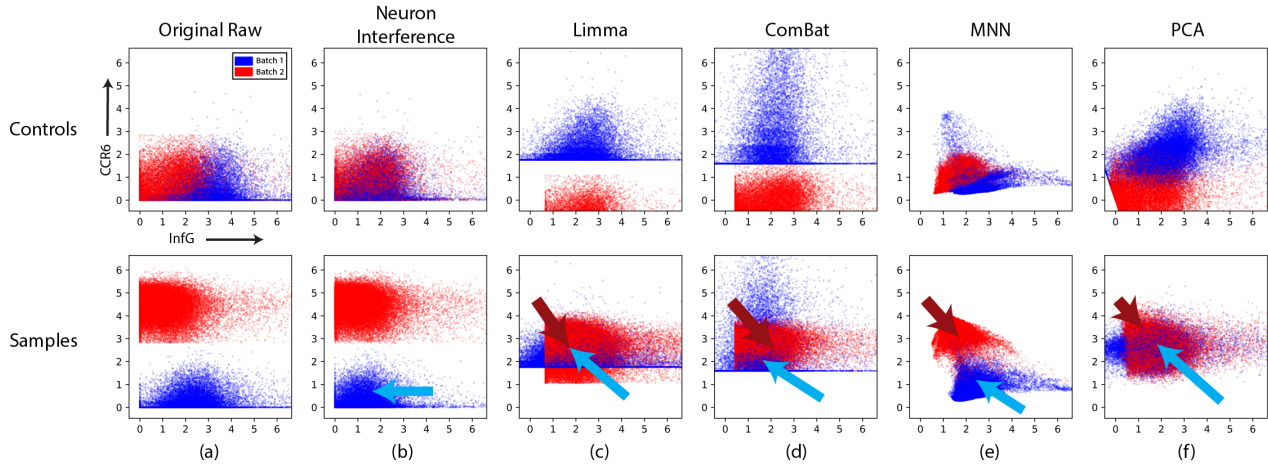


Figure 3. (a) Only horizontal variation exists between the first batch and second batch in the controls, while both horizontal and vertical variation exists in the samples (b) neuron interference identifies and corrects only the horizontal variation seen in the controls while preserving the vertical variation (c-f) other methods cannot disentangle the two sources of variation and attempt to remove all variation. The vertical/horizontal direction of batch correction applied to the sample in each method is shown with arrows.

Preserved neuron In contrast, the preserved neuron demonstrates how we can leverage the information in the controls and preserve variation that would have been removed by other methods. As seen in Figure 4, this neuron had one of the highest δ_1 values and thus was not selected for neuron interference. By looking at the activation distribution, we can see that this neuron only activates for the second batch sample, while the second batch control and both first batch distributions are at low unactivated values and very similar. Viewed on the InfG-CCR6 space, it is clear that this neuron activates for all cells high in CCR6 and only for cells high in InfG. Since this trait is seen exclusively in second batch sample cells, by not performing neuron interference on this neuron, we guarantee this signal will be preserved.

These two individual neurons demonstrate how neuron interference performs batch correction, but importantly the δ criterion prevents us from having to decide whether to remove variation neuron-by-neuron. Since the representation of each cell is distributed across all neurons, the ultimate results in Figure 3b are only achieved by correcting all neurons who meet the δ criterion.

Comparison of batch correction methods We now evaluate the results of batch correction across all dimensions comprehensively and compare to several alternative methods. Figures 3c-f show Limma [16], ComBat [17], Mutual Nearest Neighbor (MNN) [5], and batch-correlated principal component removal (PCA) [2]. Of these methods, only our neuron interference approach detects features on the full data manifold, aligns distributions non-linearly and non-parametrically, and operates piecewise on only part of the space (e.g. it lowers the InfG values for cells with high values of InfG while not shifting the InfG value for cells with low values of InfG). Since these methods do not attempt to identify and preserve any variation between batches, it is unsurprising that none differentiate between the InfG and CCR6 variation.

We note that since the data violates the parametric assumptions of some of the other methods (ComBat for example), some *introduce* batch effects where there previously were none. In the controls, the two batches were aligned perfectly along the CCR6 axis. But to match the global distributions, they were pulled apart so that afterwards the cells in the first batch are uniformly higher than all cells in the second batch. This emphasizes the importance of not using parametric models of batch effects, since they clearly affect the data in local and nonlinear ways that are difficult to model explicitly. Additionally, the samples after using ComBat show the undesirable consequences of trying to fully align the two batches. In Figure 3d, the cells with the highest CCR6 measurement end up being cells that were actually measured with very little CCR6 from the first batch, but are stretched to the very top due to the global rescaling.

In Figure 5, we expand upon the in-depth investigation of the InfG-CCR6 space and confirm that neuron interference is leveraging the evidence in the controls for all dimensions. There we see that the mean change in each marker before and after batch correction is strongly positively correlated with the difference in the controls for that dimension ($r=0.82$). Both the magnitude and the direction are well preserved, confirming that we only remove variation between batches where it has the evidence from the controls to do so.

3.3. Single-cell RNA sequencing

Finally, we consider a use of neuron interference for partially aligning batches when identical, repeatedly measured controls are not available. For this dataset, we performed a single-cell RNA sequencing experiment where a patient’s blood and cerebro-spinal fluid was sequenced before (first batch) and after (second batch) treatment. One consequence of the treatment is the depletion of B cells, so while there is technical variation between the batches, there is also known to be true biological variation. No control was measured alongside each batch, but here we illustrate how we can still use neuron interference to only remove the technical variation where there is evidence to do so, preserving the biological signal.

To compensate for the lack of known controls, we work under the *a priori* assumption that there is a subset of cells our treatment will not significantly affect, here CD4+ cells. The raw data was processed with log normalization, library size normalization, cell filtering with fewer than 300 gene counts, gene filtering on those with reads from fewer than 5 cells, and then clustering with Seurat [18]. Each cluster was matched to a cell phenotype and CD4+ cells were used as controls. The data ultimately fed into the model was in 14244 dimensions and the number of cells was 433, 862, 640, and 825 for the samples of the first and second batch and controls of the first and second batch, respectively.

In Figure 6a, we see that the CD4+ cells from the first and second batch are systematically different from each other using a TSNE embedding [19], with a similar difference between batches being visible in the CD8+ region of the embedding. In contrast, as expected the B cells come only from the first batch. By using neuron interference, we learn from the differences seen in the CD4+ cells from each batch and remove those differences (and only those differences) from all cells. As shown in Figure 6b, this successfully aligns not only the CD4+ cells, but also successfully mixes the CD8+ cells of each batch. Crucially, though, our ability to use the controls allow us to not alter the B cells even though they are exclusively seen in the first batch.

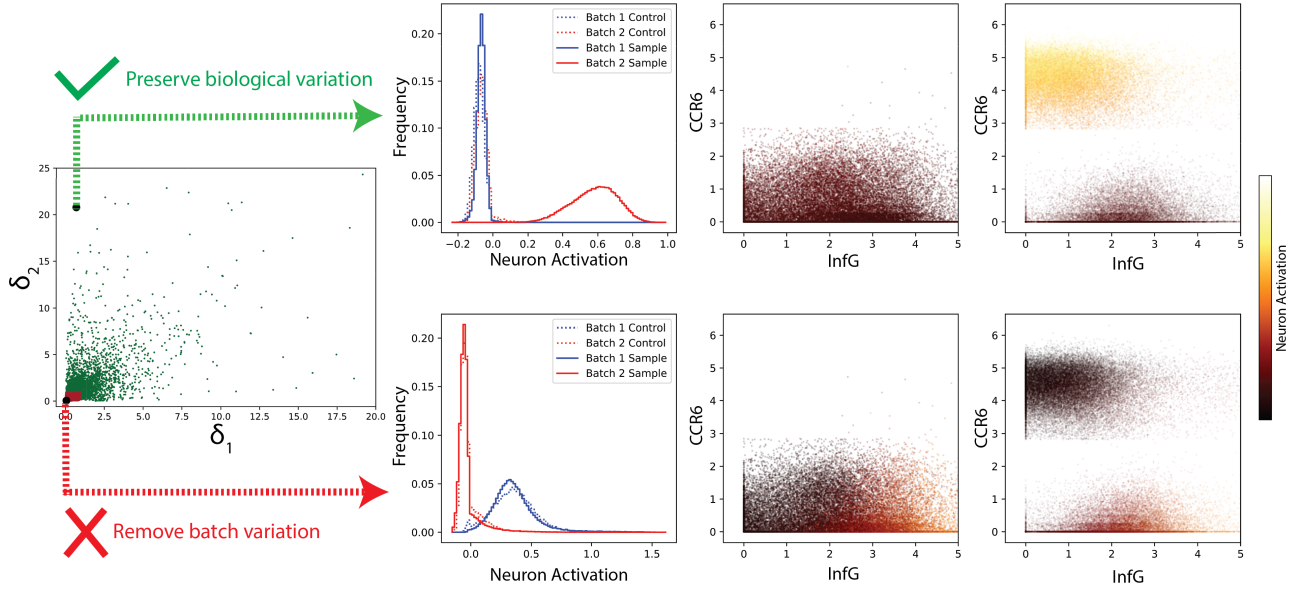


Figure 4. An archetypal preserved neuron (green) and an archetypal corrected neuron (red), as identified by our criterion. In the preserved neuron, the two controls’ histograms are identical and the neuron detects a feature that is seen exclusively in just one sample. In the corrected neuron, the detected feature exists nearly identically within the control and sample for each batch.

4. Discussion

Methods for batch correction can be broadly divided into two categories: (a) those that try to align the distributions of each batch but generally eliminate most variation beyond alignment, and (b) those that try to explicitly model the batch effects and then remove variation based on the fitted model. Our model fits most appropriately under the (b) category, as we define batch effects using control samples that are either generated for calibration, or identified using known biology. To the best of our knowledge, very few methods leverage this information in creating a model of the batch variation.

The most obvious way of using a neural network for this task is to explicitly map or align from batch to batch as in [20] or [21]. This approach eliminates all variation between samples (including biological ones) unless trained on control samples that are consistent between batches. However, if only trained on controls, then this approach cannot generalize to non-controls. By contrast, we use a simple autoencoder that recreates input data and identify neurons within the network that encode for batch differences based on an intuitive δ -criterion. These neurons encode a complex and non-linear model of the batch effects in their activation states. We then explicitly shift the activations of these neurons in a process that we term neuron interference.

Neuron interference itself can be a widely useful process for crossing features between samples or constraining them

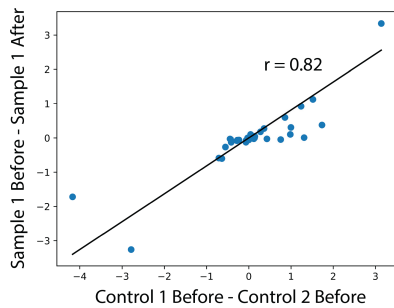


Figure 5. For each dimension, the mean change before and after batch correction is strongly correlated with the mean difference between the controls, confirming we only correct differences between batches where we have evidence to do so.

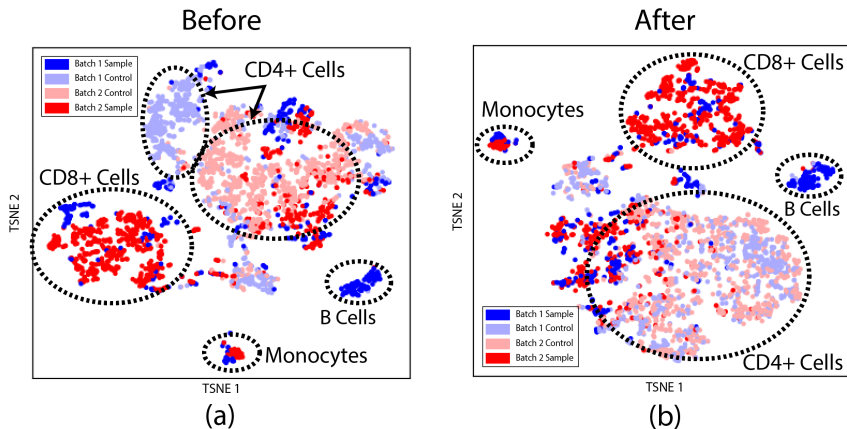


Figure 6. Neuron interference in an experiment where we take a subset of cells not expected to change with the experimental condition as controls. Here, we learn the differences between batches from just CD4+ cells, which allows us to preserve subpopulations known only to exist in one batch (like B cells).

within a dataset. This can be useful in many circumstances where different features are reliably measured in different data points. Being an inference method rather than a training one, any phenomenon that is difficult to formulate differentiably is a promising application for neuron interference. In the case presented here, we removed a particular kind of variation only if that variation is also present in a control population. We are not able to write a differentiable, analytic formulation for this notion, yet through neuron interference we are able to achieve it nevertheless.

References

[1] Jacob H Levine, Erin F Simonds, Sean C Bendall, Kara L Davis, D Amir El-ad, Michelle D Tadmor, Oren Litvin, Harris G Fienberg, Astraea Jager, Eli R Zunder, et al. Data-driven phenotypic dissection of aml reveals progenitor-like cells that correlate with prognosis. *Cell*, 162(1):184–197, 2015.

[2] Jeffrey T Leek, Robert B Scharpf, Héctor Corrada Bravo, David Simcha, Benjamin Langmead, W Evan Johnson, Donald Geman, Keith Baggerly, and Rafael A Irizarry. Tackling the widespread and critical impact of batch effects in high-throughput data. *Nature Reviews Genetics*, 11(10):733, 2010.

[3] J Luo, M Schumacher, A Scherer, D Sanoudou, D Megherbi, T Davison, T Shi, W Tong, L Shi, H Hong, et al. A comparison of batch effect removal methods for enhancement of prediction performance using maqc-ii microarray gene expression data. *The pharmacogenomics journal*, 10(4):278, 2010.

[4] Andrew Butler and Rahul Satija. Integrated analysis of single cell transcriptomic data across conditions, technologies, and species. *bioRxiv*, page 164889, 2017.

[5] Laleh Haghverdi, Aaron TL Lun, Michael D Morgan, and John C Marioni. Batch effects in single-cell rna-sequencing data are corrected by matching mutual nearest neighbors. *Nature biotechnology*, 2018.

[6] Cosmin Lazar, Stijn Meganck, Jonatan Taminau, David Steenhoff, Alain Coletta, Colin Molter, David Y Weiss-Solís, Robin Duque, Hugues Bersini, and Ann Nowé. Batch effect removal methods for microarray gene expression data integration: a survey. *Briefings in bioinformatics*, 14(4):469–490, 2012.

[7] Po-Yuan Tung, John D Blischak, Chiaowen Joyce Hsiao, David A Knowles, Jonathan E Burnett, Jonathan K Pritchard, and Yoav Gilad. Batch effects and the effective design of single-cell gene expression studies. *Scientific reports*, 7:39921, 2017.

[8] Maren Buttner, Zhichao Miao, Alexander Wolf, Sarah A Teichmann, and Fabian J Theis. Assessment of batch-correction methods for scRNA-seq data with a new test metric. *bioRxiv*, page 200345, 2017.

[9] Aaron TL Lun, Fernando J Calero-Nieto, Liora Haim-Vilmovsky, Berthold Göttgens, and John C Marioni. Assessing the reliability of spike-in normalization for analyses of single-cell rna sequencing data. *Genome research*, 27(11):1795–1806, 2017.

[10] Allon Wagner, Aviv Regev, and Nir Yosef. Revealing the vectors of cellular identity with single-cell genomics. *Nature biotechnology*, 34(11):1145, 2016.

[11] Nicola K Wilson, David G Kent, Florian Buetner, Mona Shehata, Iain C Macaulay, Fernando J Calero-Nieto, Manuel Sánchez Castillo, Caroline A Odedkoven, Evangelia Diamanti, Reiner Schulte, et al. Combined single-cell functional and gene expression analysis resolves heterogeneity within stem cell populations. *Cell stem cell*, 16(6):712–724, 2015.

[12] Katja Kleinsteuber, Björn Corleis, Narges Rashidi, Nzuekoh Nchinda, Antonella Lisanti, Josalyn L Cho, Benjamin D Medoff, Douglas Kwon, and Bruce D Walker. Standardization and quality control for high-dimensional mass cytometry studies of human samples. *Cytometry Part A*, 89(10):903–913, 2016.

[13] Xiaowei Xu, Yukun Ding, Sharon Xiaobo Hu, Michael Niemier, Jason Cong, Yu Hu, and Yiyu Shi. Scaling for edge inference of deep neural networks. *Nature Electronics*, 1(4):216, 2018.

[14] Geoffrey E Hinton and Ruslan R Salakhutdinov. Reducing the dimensionality of data with neural networks. *science*, 313(5786):504–507, 2006.

[15] Elizaveta Levina and Peter Bickel. The earth mover’s distance is the mallows distance: Some insights from statistics. In *Computer Vision, 2001. ICCV 2001. Proceedings. Eighth IEEE International Conference on*, volume 2, pages 251–256. IEEE, 2001.

[16] Jeffrey T Leek, W Evan Johnson, Hilary S Parker, Andrew E Jaffe, and John D Storey. The sva package for removing batch effects and other unwanted variation in high-throughput experiments. *Bioinformatics*, 28(6):882–883, 2012.

[17] W Evan Johnson, Cheng Li, and Ariel Rabinovic. Adjusting batch effects in microarray expression data using empirical bayes methods. *Biostatistics*, 8(1):118–127, 2007.

[18] Andrew Butler, Paul Hoffman, Peter Smibert, Efthymia Papalex, and Rahul Satija. Integrating single-cell transcriptomic data across different conditions, technologies, and species. *Nature Biotechnology*, 2018.

[19] Laurens van der Maaten and Geoffrey Hinton. Visualizing data using t-sne. *Journal of machine learning research*, 9(Nov):2579–2605, 2008.

[20] Uri Shaham, Kelly P Stanton, Jun Zhao, Huamin Li, Khadir Raddassi, Ruth Montgomery, and Yuval Kluger. Removal of batch effects using distribution-matching residual networks. *Bioinformatics*, 33(16):2539–2546, 2017.

[21] Matthew Amodio and Smita Krishnaswamy. Magan: Aligning biological manifolds. *arXiv preprint arXiv:1803.00385*, 2018.